Biomimetic Macrocyclic Inhibitors of Human Cathepsin D

Radka Houštecká[1], Lucie Marešová[-1], Martin Hadzima[1], Jindřich Fanfrlík[1], Jiří Brynda[1], Lenka Pallová[1], Iva Hánová[1], Martin Lepšík[1], Martin Horn[1], Martin Smrčina[2], Pavel Majer[1], and Michael Mareš[1]

[1]*Institute of Organic Chemistry and Biochemistry of the Czech Academy of Sciences, Prague, Czech Republic;*
[2]*Icagen Inc., Tucson Research Center, Oro Valley, USA*

Introduction

Human cathepsin D (CatD), a pepsin-family aspartic protease, plays an important role in tumor progression and metastasis. Here, we report the development of biomimetic inhibitors of CatD as novel tools for regulation of this therapeutic target. We designed a macrocyclic scaffold to mimic the spatial conformation of the minimal pseudo-dipeptide binding motif of pepstatin A, a microbial oligo-peptide inhibitor, in the CatD active

site. A library of more than 30 macrocyclic peptidomimetic inhibitors was employed for scaffold optimization, mapping of subsite interactions, and profiling of inhibitor selectivity. Furthermore, we solved high-resolution crystal structures of three macrocyclic inhibitors with low nanomolar or subnanomolar potency in complex with CatD and determined their binding mode using quantum chemical calculations. The study provides a new structural template and functional profile that can be exploited for design of potential chemotherapeutics that specifically inhibit CatD and related aspartic proteases.
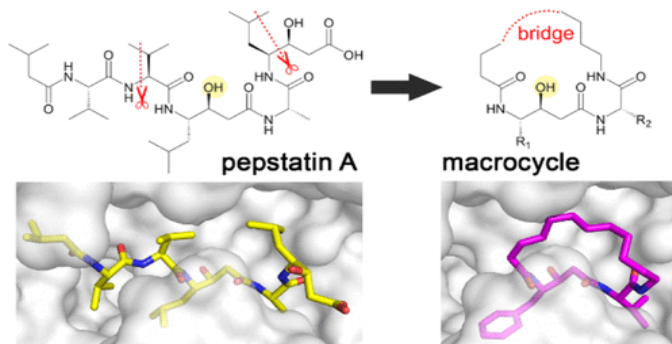
Results and Discussion

- We designed and synthesized a set of macrocyclic peptidomimetic inhibitors that were used for analysis of the macrocyclic scaffold and specificity of S1 and S2′ subsites of HCD (Figure 1).
- The high resolution crystal structures of three macrocyclic inhibitors in complex with HCD were determined. Their binding mode was investigated using quantum chemical calculations (Figure 2).
- The work identified a novel inhibitor scaffold and interaction hot spots that can be exploited for the rational design of specific inhibitors of HCD and related aspartic peptidases as potential chemotherapeutics (Figure 3).

The high affinity of naturally occurring pepstatin A for human CatD makes it an attractive template for biomimetic inhibitor design [1]. Here, we used the crystal structure of the CatD−pepstatin A complex and previously obtained SAR data as guides for rational design of small peptidomimetic inhibitors [2,3]. We aimed to avoid the inherent difficulties connected with use of linear peptides as therapeutics. Linear peptides suffer from poor oral absorption, short duration of action, proteolytic instability, and rapid biliary clearance. In contrast, cyclic peptidomimetics in general have better pharmacokinetic properties and are being increasingly employed in drug development [4-7].

First, we evaluated linear fragments of pepstatin A to assess size requirements for the inhibitory motif. Second, we analyzed pepstatin A bound in the active site of human CatD. The inhibitor adopts a U-shaped conformation with several side chains in positions that can be effectively connected by an aliphatic bridge to impose conformational constraint by cyclization. Based on these data, we designed a functional macrocyclic scaffold with minimized size. High-resolution crystal structures of CatD−macrocycle complexes revealed that this scaffold stabilizes the active site conformation seen in pepstatin A and forms a comparable number of atomic contacts and hydrogen bonds as the larger structure of the parent ligand. Quantum chemical calculations of the interaction energies of

macrocycles demonstrated the critical role of the statin residue, which is correctly positioned in the scaffold to interact with the enzyme catalytic center. The results of the structural analysis are in line with findings that proteases recognize peptide ligands with extended β-strand conformation and that this extended-like conformation can be induced in short peptides by macrocyclization to improve their affinity [8,9].
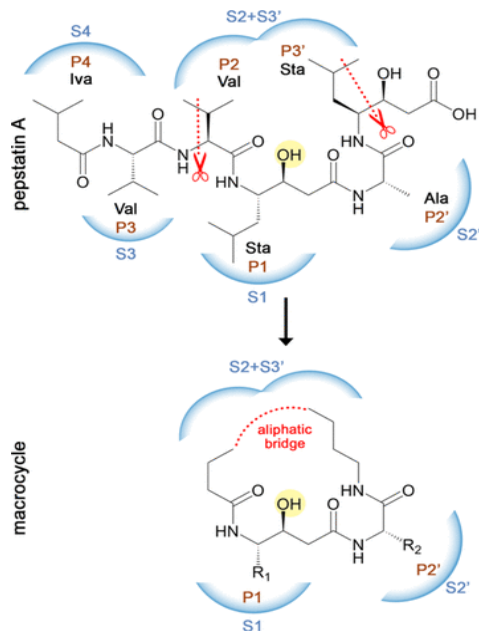
Fig. 1. Schematic representation of the rational design of the macrocyclic inhibitor scaffold. The scaffold mimics the spatial conformation of pepstatin A, a natural linear oligopeptide inhibitor, in the active site of human CatD (PDB: 1LYB). Binding subsites (S) are marked and colored in blue; corresponding inhibitor positions (P) are in brown. The central hydroxyl group of the statine residue that interacts with the catalytic aspartates of CatD is highlighted in yellow. Lines with scissors indicate the region used for macrocycle scaffold design. Pepstatin A structure: Iva-Val-Val-Sta-Ala-Sta, where Iva is isovaleryl and Sta is statine.

We prepared a library of more than 30 macrocyclic compounds (Table 1) with variable bridge size and various side chains in the P1 and P2′ positions. SAR analysis revealed that the minimized scaffold effectively potentiates inhibition, and we identified human CatD inhibitors with low nanomolar and subnanomolar potency. The inhibitor selectivity can be altered by residue substitutions in macrocycles to preferentially target human CatD or its close homologues from the A1 family of aspartic proteases. Notably, the developed compounds display favorable drug-like properties comparable to those reported for other medicinally relevant macrocycles [4-7]. They meet Lipinski's "rule of five" criteria and other physicochemical parameters for drug design that pepstatin A generally does not. Furthermore, the macrocycles are proteolytically stable and noncytotoxic, and parameters such as solubility and cell permeability can be controlled by structural substitutions. In conclusion, we present new biomimetic macrocyclics as a powerful template for further optimization and future development of potential chemotherapeutics against pathologies associated with human CatD and CatD-like proteases.
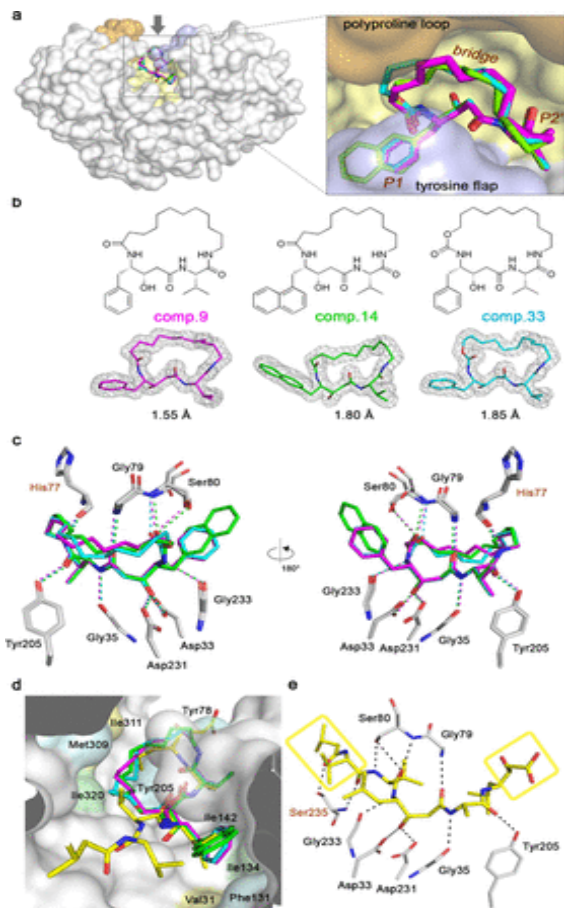
Fig. 2. Crystal structures of human CatD in complex with three macrocyclic inhibitors (**9**, **14**, and **33**, PDB codes 6QCB, 6QBG, and 6QBH). (**a**) Top view of the CatD active site with the superimposed macrocyclic inhibitors. The enzyme is shown as semitransparent surface and the inhibitors as sticks (**9**, magenta; **14**, green; **33**, cyan). The active site residues are colored as follows: Tyr flap residues are pale blue, polyproline loop residues are pale orange, and the rest of the residues are light yellow. (b) Chemical structures and electron density maps of macrocyclic inhibitors. The $2F_o$ - F_c maps are contoured at 1.2σ. (c) Hydrogen bond networks (dashed lines) formed between CatD and macrocyclic inhibitors are shown in two views rotated by 180°. Inhibitors are colored as in (b); interacting enzyme residues are gray. Heteroatoms have standard color coding. (d) Superposition of macrocyclic inhibitors colored as in (b) and pepstatin A (yellow) in the CatD active site. The enzyme is in semitransparent surface representation, and residues that form hydrophobic interactions with inhibitors are highlighted. The residues interacting with the macrocycles are pale cyan, with pepstatin A are yellow, and with both inhibitors are pale green. (e) Hydrogen bond network (dashed lines) formed between CatD and pepstatin A. Pepstatin A is colored yellow; interacting enzyme residues are gray. Yellow boxes indicate segments of pepstatin A that are absent in the macrocycle scaffold. Residues labeled in brown form pepstatin A-specific hydrogen bonds; macrocycle-specific hydrogen bonding is labeled in (c).
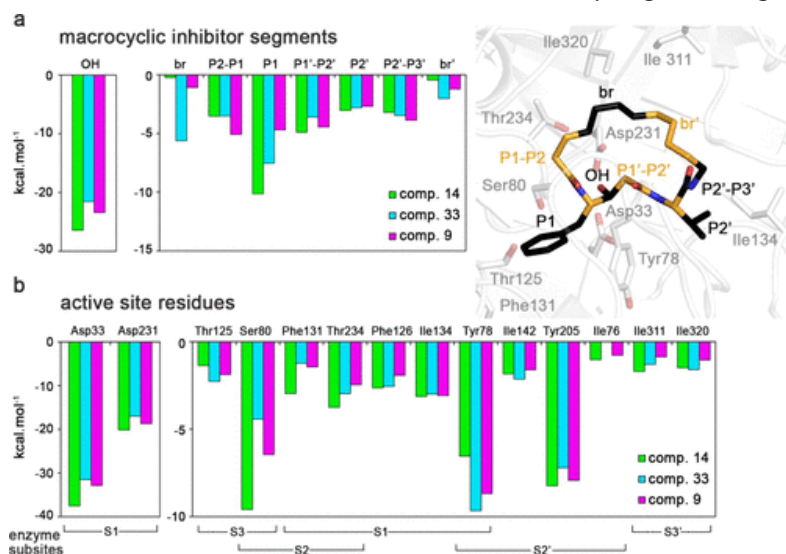
Fig. 3. Quantum chemical calculations of interaction "free" energies of three crystallographically characterized macrocyclic inhibitors in the CatD active site. The 3D view shows fragmentation of an inhibitor into segments (alternating black and orange) and the active site residues of CatD (gray) used for the calculations (PDB code 6QCB). (a) Contributions of individual inhibitor segments. (b) Contributions of the active site residues obtained from a "virtual glycine" scan.

Table 1. Substitution Analysis of Macrocyclic Inhibitors of Human CatD. Compounds with variation at the R_1 substituent (a) and the R_2 substituent (b) are ordered according to their potency.

a

Compound	R_1	IC_{50} (nM)
14		0.6 ± 0.1
15		3.1 ± 0.6
16		4.2 ± 0.7
17		4.7 ± 0.7
9		5.8 ± 0.7
18		9.0 ± 0.7
19		20 ± 4
7		22 ± 5
20		39 ± 9
21		55 ± 5
22		190 ± 20
23		340 ± 38
24		600 ± 145

b

Compound	R_2	IC_{50} (nM)
25		1.1 ± 0.2
26		3.8 ± 0.7
9		5.8 ± 0.7
27		8.2 ± 0.7
28		15 ± 3
29		16 ± 1
30		27 ± 3
8		68 ± 16
31		500 ± 55
32		560 ± 130

Acknowledgments

References

1. Knight, C.G. *Biochem. J.* **155**, 117-125 (1976), http://dx.doi.org/10.1042/bj1550117
2. Majer, P. *Protein Sci.* **6**, 1458-1466 (1997), http://dx.doi.org/10.1002/pro.5560060710
3. Baldwin, E.T. *Proc. Natl. Acad. Sci. U.S.A.* **90**, 6796-6800 (1993), http://dx.doi.org/10.1073/pnas.90.14.6796
4. Cummings, M.D. *J. Med. Chem.* **62**, 6843-6853 (2019), http://dx.doi.org/10.1021/acs.jmedchem.8b01985
5. Giordanetto, F. *J. Med. Chem.* **57**, 278-295 (2014), http://dx.doi.org/10.1021/jm400887j
6. Marsault, E. *J. Med. Chem.* **54**, 1961-2004 (2011), http://dx.doi.org/10.1021/jm1012374
7. Mallinson, J. *Future Med. Chem.* **4**, 1409-1438 (2012), http://dx.doi.org/10.4155/fmc.12.93
8. Tyndall, J. *Curr. Med. Chem.* **8**, 893-907 (2001), http://dx.doi.org/10.2174/0929867013372715
9. Madala, P.K. *Chem. Rev.* **110**, PR1-PR31 (2010), http://dx.doi.org/10.1021/cr900368a